

## Changes in dielectric properties at 460 kHz of kidney and fat during heating: importance for radio-frequency thermal therapy

Mihaela Pop<sup>1,4</sup>, Andrea Molckovsky<sup>1</sup>, Lee Chin<sup>1,4</sup>, Michael C Kolios<sup>1,5</sup>,  
Michael A S Jewett<sup>3,4</sup> and Michael D Sherar<sup>1,2,4</sup>

<sup>1</sup> Department of Medical Biophysics, University of Toronto, 610 University Avenue, Toronto, Ontario, M5G 2M9, Canada

<sup>2</sup> Department of Radiation Oncology, University of Toronto, 610 University Avenue, Toronto, Ontario, M5G 2M9, Canada

<sup>3</sup> Department of Surgery (Division of Urology), University of Toronto, 610 University Avenue, Toronto, Ontario, M5G 2M9, Canada

<sup>4</sup> Ontario Cancer Institute/Princess Margaret Hospital, 610 University Avenue, Toronto, Ontario, M5G 2M9, Canada

<sup>5</sup> Department of Mathematics, Physics and Computer Science, Ryerson University, 350 Victoria Street, Toronto, Ontario, M5B 2K3, Canada

Received 7 March 2003

Published 22 July 2003

Online at [stacks.iop.org/PMB/48/2509](http://stacks.iop.org/PMB/48/2509)

### Abstract

We have developed a system to measure the changes due to heating to high temperatures in the dielectric properties of tissues in the radio-frequency range. A two-electrode arrangement was connected to a low-frequency impedance analyser and used to measure the dielectric properties of *ex vivo* porcine kidney and fat at 460 kHz. This frequency was selected as it is the most commonly used for radio-frequency thermal therapy of renal tumours. Tissue samples were heated to target temperatures between 48 and 78 °C in a hot water bath and changes in dielectric properties were measured during 30 min of heating and 15 min of cooling. Results suggest a time–temperature dependence of dielectric properties, with two separate components: one a reversible, temperature-dependent effect and the other a permanent effect due to structural events (e.g. protein coagulation, fat melting) that occur in tissues during heating. We calculated temperature coefficients of  $1.3 \pm 0.1\% \text{ } ^\circ\text{C}^{-1}$  for kidney permittivity and  $1.6\% \text{ } ^\circ\text{C}^{-1}$  for kidney conductivity,  $0.9 \pm 0.1\% \text{ } ^\circ\text{C}^{-1}$  for fat permittivity and  $1.7 \pm 0.1\% \text{ } ^\circ\text{C}^{-1}$  for fat conductivity. An Arrhenius model was employed to determine the first-order kinetic rates for the irreversible changes in dielectric properties. The following Arrhenius parameters were determined: an activation energy of  $57 \pm 5 \text{ kcal mol}^{-1}$  and a frequency factor of  $(6 \pm 1) \times 10^{34} \text{ s}^{-1}$  for conductivity of kidney, an activation energy of  $48 \pm 2 \text{ kcal mol}^{-1}$  and a frequency factor of  $6 \times 10^{28} \text{ s}^{-1}$  for permittivity of kidney. A similar analysis led to an activation energy of  $31 \pm 4 \text{ kcal mol}^{-1}$  and a frequency factor of  $(4.43 \pm 1) \times 10^{16} \text{ s}^{-1}$  for conductivity of fat, and an

activation energy of  $40 \pm 4 \text{ kcal mol}^{-1}$  and a frequency factor of  $4 \times 10^{22} \text{ s}^{-1}$  for permittivity of fat. Structural events occurring during heating at different target temperatures as determined by histological analyses were correlated with the changes in the measured dielectric properties.

## 1. Introduction

Radio-frequency (RF) thermal therapy based on heating tumours to temperatures beyond  $50 \text{ }^\circ\text{C}$  where cell death is induced by protein coagulation (Pearce and Thomsen 1995), is currently being investigated for the treatment of renal cell carcinomas (Rendon *et al* 2001, 2002, Gervais *et al* 2000, Michaels *et al* 2002). However, the biophysical mechanisms of RF thermal lesion growth in kidney are not yet well understood. One of the unknown factors is the time–temperature dependence of dielectric properties of kidney and surrounding structures (e.g. perirenal fat) at the radio frequencies employed.

The energy absorbed from an RF source depends strongly on tissue dielectric properties (Strohbehm 1983, Van de Kamer *et al* 2001). As a result, changes in dielectric properties during heating will affect the tissue temperature distribution and the resulting thermal damage. Several numerical models for predicting the RF thermal damage in heart muscle and liver have been proposed, but they either incorporated only temperature-dependent changes in electrical conductivity (Labonté 1994) or consider the conductivity to be constant (Haemmerich *et al* 2001). Moreover, where the model included the temperature coefficient ( $+2\% \text{ }^\circ\text{C}^{-1}$ ) for the tissue electrical conductivity, the value was extrapolated from measurements made below  $42 \text{ }^\circ\text{C}$  (Schwan and Foster 1980). These approximations may lead to erroneous predictions of thermal damage.

Based on dielectric measurements at other frequencies we hypothesized that electrical conductivity and permittivity may exhibit both a reversible temperature dependence and an irreversible dependence on structural changes that occur in tissue during heating. The majority of commercial RF generators, approved for clinical use in cancer therapy, produces 460 kHz. Changes in dielectric properties at this frequency during heating to high temperatures have not been measured. We have developed a system capable of measuring the time–temperature dependence of dielectric properties of *ex vivo* tissues and applied it to porcine renal and fat tissue measurements at 460 kHz. In addition, we have correlated irreversible changes in dielectric properties of porcine kidney and fat tissue with histology. The quantitative data were then used in deriving mathematical expressions that, based on an Arrhenius-type kinetic model, can be used to predict the changes in dielectric properties due to any thermal history. These changes can be incorporated in a theoretical model to more accurately predict the temperature distribution and resulting thermal damage during RF thermal therapy in renal tissue.

## 2. Materials and methods

### 2.1. Dielectric measurement: two-terminal electrode arrangement and calibration

Dielectric properties of tissue were measured with two Teflon insulated platinum (Pt) needle electrodes mounted in parallel and inserted into the tissue specimen. Pt-electrodes were chosen because they reduce polarization effects arising at low frequencies at the interfaces between dielectric media, i.e. electrodes and tissue (Schwan 1963). At high frequencies ( $>600 \text{ kHz}$ )

stray factors (capacitive, resistive and inductive) introduce an additional impedance,  $Z_{\text{highfreq}}$ , within the measurement circuit which also affect the measurement of tissue impedance  $Z_{\text{tissue}}$ . The measured impedance,  $Z = Z_{\text{pol}} + Z_{\text{tissue}} + Z_{\text{highfreq}}$ , can be represented by a simple equivalent circuit with each impedance element comprising resistive and capacitance elements. To obtain  $Z_{\text{tissue}}$  from the measured impedance  $Z$ ,  $Z_{\text{pol}}$  and  $Z_{\text{highfreq}}$  are subtracted using a calibration procedure described later. This simple circuit model has been used to characterize the dielectric behaviour of a wide variety of biological systems (Hart and Dunfee 1993, Hart *et al* 1998, Molckovsky and Wilson 2001).

By considering a parallel equivalent capacitance and conductance circuit, the measured complex impedance,  $Z$  is related to the capacitance  $C$  and conductance  $G$  as follows (Schwan and Foster 1980, Martinsen *et al* 2002):

$$Z = \frac{G}{G^2 + \omega^2 C^2} - j \frac{\omega C}{G^2 + \omega^2 C^2} \quad (1)$$

where  $\omega = 2\pi\nu$  and  $\nu$  is the frequency of interest. The values of  $G$  and  $C$  used in equation (1) are dependent on *geometrical parameters* (tissue cross-sectional area  $A$ , and inter-electrode separation  $d$ ) and *material properties* (electrical conductivity  $\sigma$ , and relative permittivity  $\epsilon'$ ) by the following relations:

$$G = \sigma \frac{A}{d} \quad (2)$$

$$C = \epsilon' \epsilon_0 \frac{A}{d} \quad (3)$$

where  $\epsilon_0$  is the permittivity of free space. If  $G$  and  $C$  are measured using an impedance analyser, then the derivation of dielectric properties,  $\sigma$  and  $\epsilon'$ , is straightforward. For convenience, the cell constant  $K$  defined as the ratio of  $A$  and  $d$ , incorporates both these geometrical parameters for the two-electrode arrangement.  $K$  is derived from the calibration procedure to avoid errors in calculating  $A$  and  $d$  due to the small electrode dimensions.

A detailed description of the calibration procedure has been given elsewhere (Molckovsky and Wilson 2001). Briefly, dielectric spectra of 0.9% NaCl solution and an agar phantom (Kato and Ishida 1987) with known dielectric properties at 22 °C, were recorded over the frequency range of 1 kHz to 1 MHz, swept logarithmically with 20 measurement points per decade. Dielectric measurements were obtained using a low-frequency impedance analyser (model 4192A LF Hewlett-Packard, Yokogawa, Japan) under the control of LabView software (National Instruments, Austin, Texas).  $Z_{\text{pol}}$  and  $Z_{\text{highfreq}}$  were calculated by fitting the measured spectra of 0.9% NaCl solution and agar phantom to their theoretical spectra, using nonlinear least squares.  $Z_{\text{tissue}}$  was then calculated by subtracting  $Z_{\text{pol}}$  and  $Z_{\text{highfreq}}$  from  $Z$  for the recorded dielectric spectra of kidney and fat tissue (assuming the same equivalent circuit). From these corrected spectra, values for  $\sigma$  and  $\epsilon'$  were extracted at 460 kHz for the tissue specimens using equations (2) and (3). The dielectric measurements during heating employed the same measurement and control systems, with recorded data corrected using the calibration parameters.

## 2.2. Tissue preparation

Freshly excised porcine kidney cortex and peritoneal fat were used in our study. The tissues were obtained directly from an abattoir and were either used immediately or stored at 4 °C and used within a few hours.

Representative samples were obtained for histology at the end of dielectric measurements from unheated tissues and from tissues heated to each target temperature. Samples were fixed

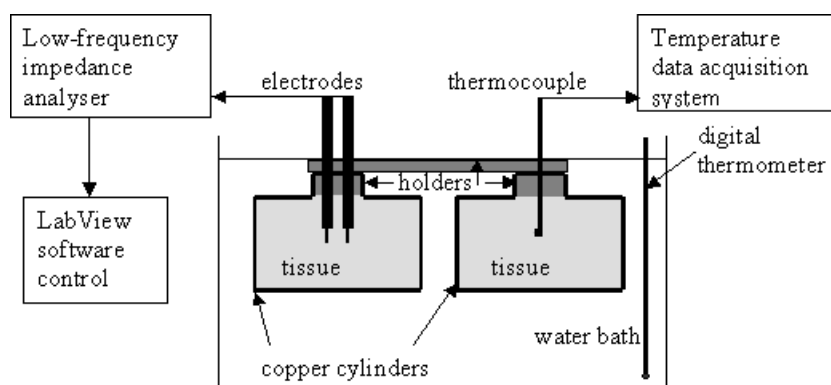


**Figure 1.** Schematic diagram of the experimental set-up.

in 10% formalin and paraffin embedded sections were stained with hematoxylin and eosin (H&E).

### 2.3. Experimental procedure and data acquisition

We employed a similar experimental protocol for dielectric property measurement to that proposed by Ryan *et al* (1997), with the exception that our electrode arrangement consisted of needle electrodes instead of end-plate electrodes. Needle electrodes were chosen because tissue shrinkage and subsequent lost of contact between tissue and end-plate electrodes can lead to erroneous data recording. Tissue samples ( $7.4 \text{ cm}^3$ ) were carefully cut and introduced into a copper cylinder (length 4.2 cm, diameter 1.5 cm). Two Pt-coated electrodes (diameter 0.25 mm) were inserted into the samples (figure 1) in the middle of the cylinder at a depth of 6 mm. This depth was chosen to be the same for all experiments in order to eliminate any variation in absolute impedance values with depth. The exposed electrode tips were 3 mm in length and located 4 mm apart.

After recording baseline spectra from tissues in a water bath maintained at  $22 \text{ }^\circ\text{C}$ , the two cylinders, fixed together within a Plexiglas holder, were transferred into a hot water bath and heated for 30 min at a specific target temperature. The samples were then quickly transferred into the cold water bath and cooled for 15 min, back at the original temperature ( $22 \text{ }^\circ\text{C}$ ). Impedance data were measured for 2–4 tissue samples at each target temperature. The electrical conductivity of 0.9% saline solution was measured over a range of temperatures (from  $22$  to  $70 \text{ }^\circ\text{C}$ ) to correct for any artefacts in the system at high temperatures. A temperature coefficient for the electrical conductivity of saline of  $(1.94 \pm 0.08)\% \text{ }^\circ\text{C}^{-1}$  was obtained from six heat-up and cool-down curves. This is in agreement with a theoretical  $+2\% \text{ }^\circ\text{C}^{-1}$  derived by Schwan and Foster (1980).

Tissue dielectric measurements at 460 kHz and temperature data were collected simultaneously, every 30 s for kidney and every 1 min for fat. The very small values for the conductance of fat tissue (order of  $\mu\text{S}$ ) made measurements extremely sensitive to correction for inductive effects occurring after immersion in the hot water bath. Therefore, the fat samples were removed for approximately 1 s from the water bath at each measurement time point to collect impedance data. The samples were then immediately re-immersed in the water bath. This rapid removal and re-immersion was not expected to result in significant cooling.

Temperature was measured via a thermocouple (type K, accuracy  $0.06 \text{ }^\circ\text{C}$ ) inserted into a second identical cylinder containing tissue, at a position corresponding to midway between

the exposed electrode tips (figure 1). This second cylinder was used to avoid artefacts in the raw impedance data when the thermocouple is inserted into the tissue between the electrodes (Ryan *et al* 1997). The thermocouple data were recorded by a Labmate Data Acquisition and Control System (Scimetric Instruments, Ottawa, Ontario) controlled by a PC. The hot water bath was maintained at different target temperatures (controlled with a digital thermometer) using a pump and another temperature controlled water bath (Haake F3, Karlsruhe, West Germany) connected in a closed loop. After reaching thermal equilibrium, the temperatures of the samples were maintained constant within  $\pm 0.3$  °C. However, due to a limitation of our heating system (loss of heat through the plastic tubing), we could achieve tissue temperatures up to approximately 80 °C only.

#### 2.4. Arrhenius analysis

If a single biological molecular species (e.g. one type of protein) is assumed to be responsible for the thermal denaturation, then the theory of first-order chemical kinetics can be applied. The thermal damage,  $\Omega$ , is defined as the logarithm of the ratio of the original concentration of native tissue at time zero,  $C(0)$ , to the remaining native state tissue at time  $t$ ,  $C(t)$ , where the rate of reaction (the change in concentration per unit time) is characterized by a rate constant,  $k$ . The Arrhenius formulation establishes a relationship between the rate of thermal damage accumulation and temperature:

$$k(T) = A \exp\left(-\frac{E_a}{RT}\right) \quad (4)$$

where  $A$  is the frequency constant ( $s^{-1}$ ),  $E_a$  is the activation energy ( $kcal\ mol^{-1}$ ),  $T$  is the temperature (K) and  $R$  is the gas constant ( $1.98\ cal\ mol^{-1}\ K^{-1}$ ).

The thermal damage ( $\Omega$ ) is then given by (Henriques 1947):

$$\Omega(t) = \ln\left\{\frac{[C(0)]}{[C(t)]}\right\} = \int_0^t A e^{-\frac{E_a}{RT(\tau)}} d\tau = \int_0^t k(T(\tau)) d\tau \quad (5)$$

where  $\Omega$  is the thermal damage index (dimensionless) and  $t$  denotes the exposure time (s). Therefore,  $\Omega = 1$  represents a state where 63% of the tissue molecules are in a *denaturated* state characterized by permanent structural changes in tissue properties, while the rest of the molecules are in their *native* state.

We have incorporated a single first-order exponential approximation into our analysis to determine the Arrhenius parameters,  $E_a$  and  $A$ , for the changes in dielectric properties of tissues caused by irreversible structural changes during heating. Similar analyses were previously used to mathematically describe the changes in optical properties of egg-white (Meijerink 1995) and rat prostate tissue (Skinner *et al* 2000), and in dielectric properties of bovine liver at 915 MHz (Chin and Sherar 2001). In this methodology the structural changes in electrical conductivity and dielectric constant, at a constant temperature  $T$ ,  $\Delta\sigma(t)$  and  $\Delta\varepsilon'(t)$ , for both tissues kidney and fat, were modelled by the following equations:

$$\Delta\varepsilon'(t) = \Delta\varepsilon' \max[1 - \exp(-k(T)t)] \quad (6)$$

$$\Delta\sigma(t) = \Delta\sigma \max[1 - \exp(-k(T)t)] \quad (7)$$

where  $\Delta\varepsilon'(t) = \varepsilon'(t) - \varepsilon'_{\text{native}}$  and  $\Delta\sigma(t) = \sigma(t) - \sigma_{\text{native}}$  are definitions necessary in describing the temporal changes in  $\varepsilon'$  and  $\sigma$ , relative to the values  $\varepsilon'_{\text{native}}$  and  $\sigma_{\text{native}}$  corresponding to the *native* state. For convenience, we also introduce the notation  $\varepsilon'_{\text{denaturated}}$  and  $\sigma_{\text{denaturated}}$  corresponding to the values of the dielectric properties in the fully *denaturated* state of tissue

(e.g. the kidney tissue is completely coagulated). Thus, when the denaturation process is complete, a value describing the maximum change in each dielectric property can be defined as  $\Delta\varepsilon'_{\max} = \varepsilon'_{\text{denaturated}} - \varepsilon'_{\text{native}}$  and  $\Delta\sigma_{\max} = \sigma_{\text{denaturated}} - \sigma_{\text{native}}$ , respectively. By fitting the experimental datasets  $\Delta\varepsilon'(t)$  and  $\Delta\sigma(t)$  to equations (6) and (7), the rate constants at each target temperature  $k(T)$  were determined.

According to equation (4), a plot of the logarithm of the rate constant versus the reciprocal of the absolute temperature will produce a straight line, where  $E_a$  and  $A$  can be determined from the slope and the intercept, respectively. Having found the Arrhenius parameters, a critical temperature  $T_{\text{crit}}$ , can be calculated as the temperature at which the tissue has denaturated to a fraction of 0.63 relative to its native state (Pearce and Thomsen 1995):

$$T_{\text{crit}} = \frac{E_a}{R \ln(A)}. \quad (8)$$

Given the exponential nature of  $\Omega$ , the rate of damage accumulation  $d\Omega/dt$ , below  $T_{\text{crit}}$  is small but increases rapidly beyond it. Therefore, the critical temperature is a useful threshold temperature for planning thermal therapy. However, using Arrhenius parameters  $E_a$  and  $A$  (equation (5)), one can predict the permanent (irreversible) structural changes in dielectric properties as a result of any thermal history.

### 3. Results

#### 3.1. Relative permittivity and electrical conductivity measurements

Measurements were first performed at a baseline temperature of 22 °C. The values derived were  $(3.21 \pm 0.11) \times 10^3$  ( $\varepsilon'$ , renal tissue) and  $0.22 \pm 0.01 \text{ Sm}^{-1}$  ( $\sigma$ , renal tissue),  $43.06 \pm 2.04$  ( $\varepsilon'$ , fat) and  $(19.98 \pm 1.36) \times 10^{-3} \text{ Sm}^{-1}$  ( $\sigma$ , fat), where the errors represent standard errors of the mean of a set of 22 samples of renal tissue, and 17 samples of fat tissue, respectively. These values are consistent with those compiled by Gabriel *et al* (1996) and Schwan and Foster (1980) below 1 MHz and at temperatures between 20 and 22 °C.

In the heated tissue experiments, the following steady state temperatures were achieved: 48.4 °C, 55.1 °C, 60.2 °C, 64.3 °C, 68.2 °C, 74.2 °C, 78.5 °C for kidney tissue and 48.5 °C, 60.3 °C, 68.1 °C, 71.3 °C, 78.4 °C for fat tissue. Results from a total of 22 experiments for kidney and 17 for fat tissue are presented.

Figures 2 and 3 show  $\varepsilon'$  and  $\sigma$  for renal tissue during heating and subsequent cooling. To account for biological variability in native tissue properties, data from each sample were normalized to its own baseline value at time  $t = 0$  min. From the temperature history (not shown here) tissue samples were seen to reach 95% of the target temperatures in about 4–6 min.

An initial sharp increase in  $\varepsilon'$  by up to 39% followed by a decrease during the remaining heating time was observed (figure 2). The decrease is not evident below the coagulation threshold and therefore it is likely due to irreversible structural changes. As the target temperature increases the maximum value of  $\varepsilon'$  decreases, probably because coagulation starts to occur before the samples reach thermal equilibrium. During the cooling period of 15 min, permittivity decreased until the samples reached room temperature (22 °C), but thereafter remained constant till the end of the cooling period. Changes in  $\varepsilon'$  during heating were partially irreversible since the final values in  $\varepsilon'$  at the end of the cooling period were found to be smaller than the values before heating. These results suggest that the initial rise in  $\varepsilon'$  is due to temperature only and is not time dependent, whereas the subsequent decrease in  $\varepsilon'$  during heating is due to irreversible structural changes that occur in tissue as a function of time during heating.

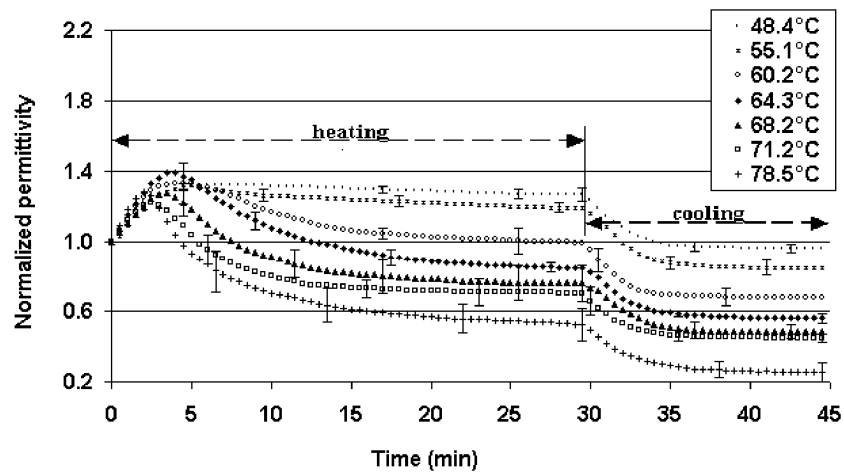


**Figure 2.** Changes in normalized relative permittivity of porcine kidney at 460 kHz, as a function of heating and cooling time for a range of temperatures indicated in the legend (for each temperature, the mean of typically 2–4 datasets  $\pm$  representative SD are plotted).

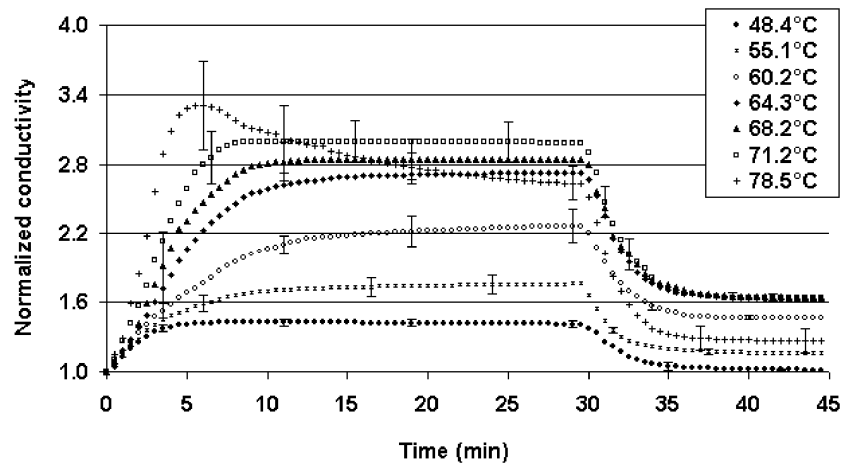


**Figure 3.** Changes in normalized conductivity of porcine kidney at 460 kHz, as a function of heating and cooling time for a range of temperatures indicated in the legend (for each temperature, the mean of typically 2–4 datasets  $\pm$  representative SD are plotted).

The conductivity of renal tissue increased rapidly initially with larger slopes for higher target temperatures (figure 3). This rise was followed by a more gradual increase after the samples reached thermal equilibrium. At high temperatures, the transition to the slower rate of increase in conductivity occurred at earlier times than at low temperatures. For the samples exposed to temperatures between 64.3 and 71.2 °C, conductivity values reached a plateau 2.7–3.0 times greater than native values. In contrast, the conductivity of the samples heated at 78.5 °C increased sharply and then started to decrease continuously such that, at the end of the heating time,  $\sigma$  was smaller than the values measured between 64.3 and 71.2 °C. The aberrant behaviour of tissue heated to the highest target temperature was attributed to desiccation (gross inspection of samples heated to 78.5 °C revealed they had shrunk by approximately 15% in

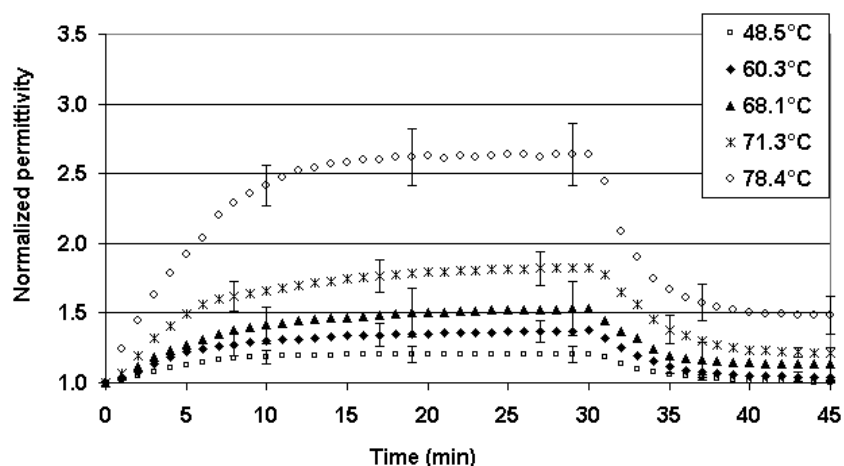


**Figure 4.** Changes in normalized relative permittivity of porcine fat at 460 kHz, as a function of heating and cooling time for a range of temperatures indicated in the legend (for each temperature, the mean of typically 2–4 datasets  $\pm$  representative SD are plotted).

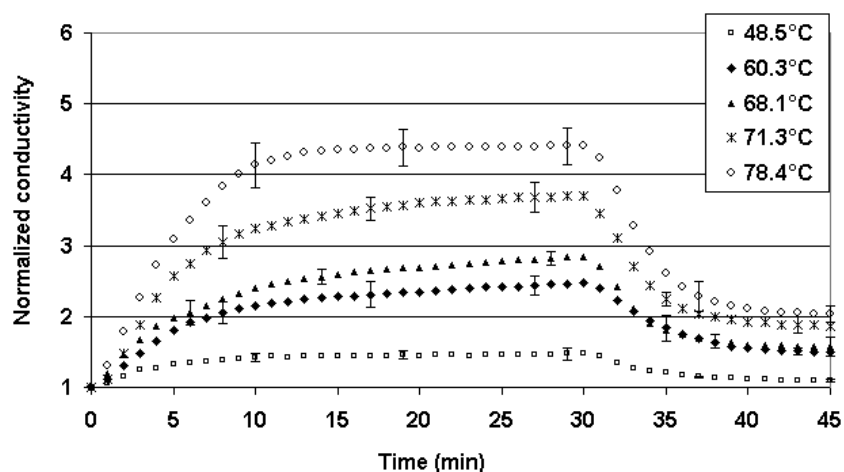


**Figure 5.** Changes in normalized relative conductivity of porcine fat at 460 kHz, as a function of heating and cooling time for a range of temperatures indicated in the legend (for each temperature, the mean of typically 2–4 datasets  $\pm$  representative SD are plotted).

volume). During the cooling period,  $\sigma$  decreased to a conductivity value that was greater than for native tissue. In particular, samples heated between 64.3 and 71.2 °C return to values all similar (average factor 1.63). After cooling, the samples heated at 78.5 °C were noted to be less conductive than the samples exposed to temperatures in the range 60.2–71.2 °C.

Figures 4 and 5 show the changes in dielectric properties of fat tissue over the 30 min of heating and the subsequent cooling period. In contrast to renal tissue, permittivity and conductivity of fat tissue exhibit similar behaviour, both sharply increasing initially, followed by a slower gradual increase. Comparing values at the end of the heating period to native values for target temperatures between 48.5 and 71.3 °C,  $\epsilon'$  increased by a factor of up to 1.8, whereas  $\sigma$  increased by a factor of nearly 4. Dielectric properties of fat reached a plateau only at the highest target temperature (78.4 °C), where the value of  $\epsilon'$  increased by a factor of 2.7,

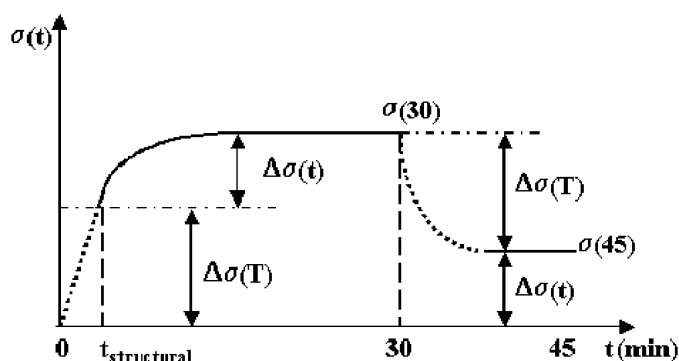


**Figure 6.** Schematic diagram for separation of temperature effect from structural effect in changes in  $\sigma(t)$ . The time point  $t_{\text{structural}}$  separates the changes in  $\sigma(t)$  due to the *reversible* temperature effect (dotted line) from the *permanent* structural effect (line).

and value of  $\sigma$  increased by a factor of 4.4, relative to baseline values. During the cooling period, both  $\epsilon'$  and  $\sigma$  of fat decreased to values greater than the baseline values suggesting that irreversible structural changes had occurred in fat tissue during heating. The smallest permanent changes in dielectric properties of fat were observed in samples heated to the lowest temperature (48.5 °C).

### 3.2. Separation of reversible and irreversible dielectric changes

The dielectric properties of both kidney and fat tissue exhibit a time–temperature dependence that can be modelled as two separate processes: a reversible temperature-dependent effect, and a permanent effect due to structural changes that occur during heating. In the case of kidney tissue, the shift of the peak measurement of  $\epsilon'$  to earlier times suggested that the structural changes started to manifest before the thermal equilibrium was reached. A separation of *temperature effect* from the *structural effect* (independent of temperature) during this stage of the experiment is therefore subject to inaccuracies. However, the ratio between the values of the dielectric properties at the end of heating time ( $t = 30$  min) and the values at the end of cooling time ( $t = 45$  min),  $\epsilon'(30)/\epsilon'(45)$  and  $\sigma(30)/\sigma(45)$ , gives the relative changes  $\Delta\epsilon'(T)$  and  $\Delta\sigma(T)$  due to temperature only if we assume that negligible structural changes occurred during the cooling period.

The thermal damage started to accumulate (up to the end of the heating period of 30 min) at a time point noted  $t_{\text{structural}}$ . We assumed that at this time point the reversible temperature effect is ‘fully’ manifested and any further changes in dielectric properties are due to the structural effect only. From the experimental curves one can subtract  $\Delta\epsilon'(T)$  and  $\Delta\sigma(T)$  from the temporal changes  $\epsilon'(t)$  and  $\sigma(t)$  (which are normalized relative to values at room temperature) and obtain the relative changes  $\Delta\epsilon'(t)$  and  $\Delta\sigma(t)$  due to the structural effects. For clarity we drew a generic diagram for  $\sigma(t)$  (figure 6). It is important to mention that the values in  $\sigma(t)$  or  $\epsilon'(t)$  corresponding to the time point  $t_{\text{structural}}$  represent the *native* (not-denatured) values used in equations (6) and (7).

**3.2.1. Temperature coefficient.** Figure 7 shows the relative changes in dielectric values,  $\epsilon'(30)/\epsilon'(45)$  and  $\sigma(30)/\sigma(45)$ , versus temperature increase. Linear regressions based on weighted least square (WLS) fittings were performed and temperature coefficients were determined from the resulting slopes (table 1).

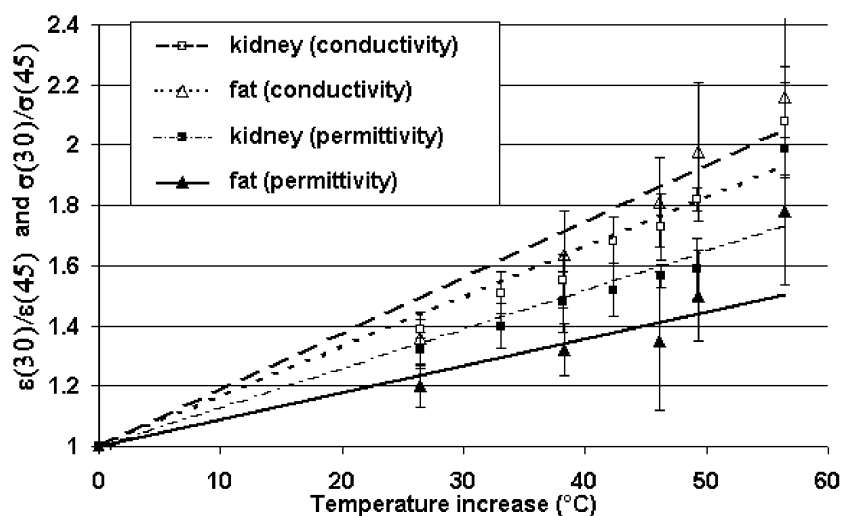


**Figure 7.** Relative changes  $\varepsilon'(30)/\varepsilon'(45)$  in permittivity of porcine kidney (■) and fat (▲), and relative changes  $\sigma(30)/\sigma(45)$  in conductivity of porcine kidney (□) and fat (△), versus the absolute increase in tissue temperature. Lines indicate linear fits of these data.

**Table 1.** Temperature coefficients for dielectric properties at 460 kHz of *ex vivo* porcine kidney and peritoneal fat (error represents standard error of the slope).

	$(\Delta\sigma/\sigma)\Delta T^{-1}$ (% °C <sup>-1</sup> )	$(\Delta\varepsilon'/\varepsilon')\Delta T^{-1}$ (% °C <sup>-1</sup> )
Porcine renal tissue, <i>ex vivo</i>	$1.62 \pm 0.04$	$1.31 \pm 0.05$
Porcine peritoneal fat, <i>ex vivo</i>	$1.71 \pm 0.12$	$0.89 \pm 0.09$

**Table 2.** Experimentally determined Arrhenius coefficients for the dielectric properties at 460 kHz of *ex vivo* porcine kidney and peritoneal fat and derived critical temperatures (error represents standard error of the slope).

Dielectric property	$A$ (s <sup>-1</sup> )	$E_a$ (kcal mol <sup>-1</sup> )	$T_{crit}$ (°C)		
			For $t = 10$ s	For $t = 10$ min	
Porcine renal tissue, <i>ex vivo</i>	$\sigma$	$(5.73 \pm 0.58) \times 10^{34}$	$57.42 \pm 5.33$	79.1	62.4
	$\varepsilon'$	$(5.85 \pm 0.23) \times 10^{28}$	$48.32 \pm 1.72$	82.9	62.8
Porcine peritoneal fat, <i>ex vivo</i>	$\sigma$	$(4.43 \pm 0.61) \times 10^{16}$	$30.79 \pm 3.52$	109.6	74.5
	$\varepsilon'$	$(3.79 \pm 0.37) \times 10^{22}$	$40.35 \pm 3.71$	102.2	75.9

**3.2.2. Arrhenius analysis.** In order to find the reaction rates,  $k(T)$ , in the analysis of the structural changes, each dataset between  $t_{structural}$  and the end of the 30 min heating period was fitted to equation (6) or (7) using nonlinear regression.

For renal tissue, data for  $\varepsilon'$  were fitted to equation (6) using an averaged value  $\Delta\varepsilon'_{max}$  as a convergence criterion in the fittings of datasets obtained at temperatures between 48.4 °C and 64.3 °C. This averaged value was calculated from the values at the end of cooling periods after heating at 68.2 °C and 71.2 °C (where  $\varepsilon'$  reached a plateau during the last 10–15 min of heating). A linear regression of  $\ln(k)$  versus  $1/T$  (figure 8), resulted in Arrhenius parameters for the changes in  $\varepsilon'$  of kidney tissue given in table 2.

Experimental datasets for  $\sigma$  were fitted to equation (7), using  $\Delta\sigma_{max}$  as a convergence criterion for temperatures up to 60.2 °C. An average experimental value of  $\Delta\sigma_{max}$  was

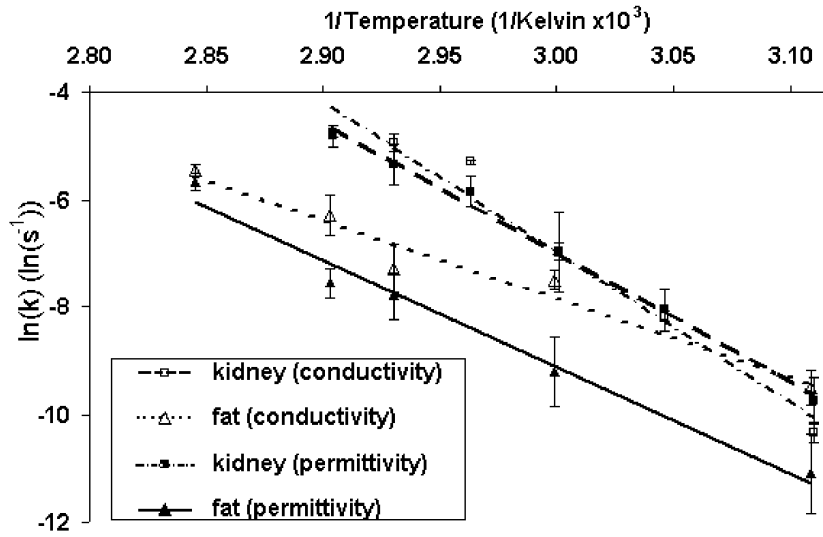


Figure 8. Arrhenius plots of  $\ln(k)$ , relative to changes in permittivity of porcine kidney (■) and fat (▲), and conductivity of porcine kidney (□) and fat (△), versus the inverse of absolute temperature,  $1/T$ . Lines indicate linear fits of these data.

calculated from the values that plateau after cooling from exposure to high temperatures 64.3–71.3 °C. Kidney dielectric data from 78.3 °C were not used in the Arrhenius analysis because the desiccation process resulting in tissue shrinkage confounded the measurements. Arrhenius parameters,  $E_a$  and  $A$  (related to the changes in  $\sigma$ ) were determined from linear regression of the plotted data (figure 8) and are included in table 2.

A similar analysis was employed to determine the Arrhenius parameters characterizing the changes in dielectric properties of fat at 460 kHz during heating. The experimental curves describing the behaviour of  $\varepsilon'$  and  $\sigma$  during heating were observed to plateau only at the highest target temperature (78.4 °C). Therefore, averaged values of  $\Delta\varepsilon'_{\max}$  and  $\Delta\sigma_{\max}$  were calculated over the four measurements performed at 78.4 °C. Arrhenius parameters derived from the slopes and intercepts of the relevant data in figure 8 are included in table 2.

Mathematical equations accounting for both effects (temperature and structural) on the dielectric properties of kidney and fat tissue can now be compiled. They are based on the temperature coefficients and the Arrhenius parameters ( $A$  and  $E_a$ ) derived in this work. These equations can then be used to describe the changes in  $\sigma(t)$  and  $\varepsilon'(t)$  as a result of any thermal history:

$$\sigma_{\text{kidney}}(t, T) = 0.22 \left\{ 1 + 0.016(T(t) - T_0) + 0.63 \left[ 1 - \exp \left( -5.73 \times 10^{34} \times \int_0^t \exp \left( -\frac{57.42 \times 10^3}{RT(\tau)} \right) d\tau \right) \right] \right\} \quad (9)$$

$$\varepsilon_{\text{kidney}}(t, T) = 3210 \left\{ 1 + 0.013(T(t) - T_0) - 0.57 \left[ 1 - \exp \left( -5.85 \times 10^{28} \times \int_0^t \exp \left( -\frac{48.32 \times 10^3}{RT(\tau)} \right) d\tau \right) \right] \right\} \quad (10)$$

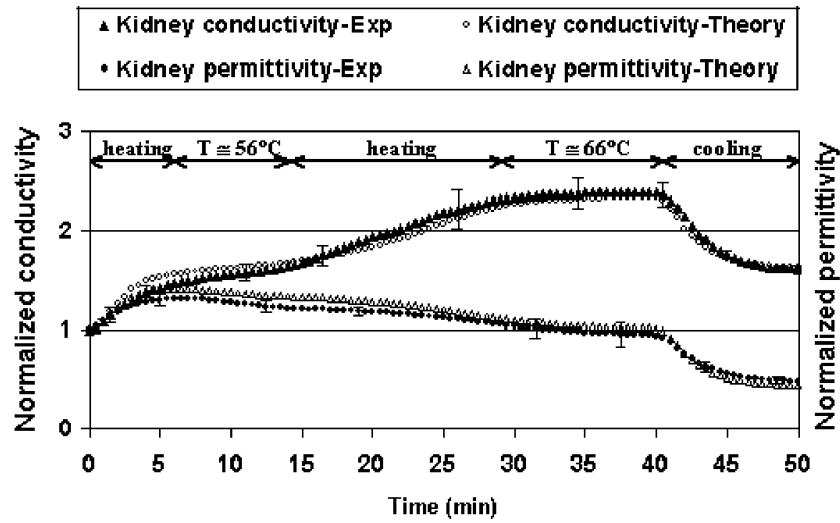


**Figure 9.** Changes in normalized experimental and normalized theoretical dielectric properties of porcine kidney: experimental permittivity (●), experimental conductivity (▲), theoretical permittivity (○) and theoretical conductivity (△) as a function of heating and cooling time (experimental curves are the average of two datasets  $\pm$  representative SD).

$$\sigma_{\text{fat}}(t, T) = 19.98 \left\{ 1 + 0.017(T(t) - T_0) + 1.04 \left[ 1 - \exp \left( -4.43 \times 10^{16} \times \int_0^t \exp \left( -\frac{30.79 \times 10^3}{RT(\tau)} \right) d\tau \right) \right] \right\} \quad (11)$$

$$\varepsilon_{\text{fat}}(t, T) = 43 \left\{ 1 + 0.009(T(t) - T_0) + 0.48 \left[ 1 - \exp \left( -3.79 \times 10^{22} \times \int_0^t \exp \left( -\frac{40.35 \times 10^3}{RT(\tau)} \right) d\tau \right) \right] \right\} \quad (12)$$

where  $T_0 = 22$  °C,  $R$  is the gas constant ( $1.98 \text{ cal mol}^{-1} \text{ K}^{-1}$ ),  $t$  denotes the exposure time and  $T(t)$  is the thermal history of the tissue (K).

Critical temperatures necessary to induce 0.63 of complete thermal damage in each tissue in 10 s and 10 min, were calculated using equation (8) and are given in table 2.

To test the above equations, a different time/temperature experiment was performed. Kidney samples were heated to approximately 56 °C for 6 min, then heated to approximately 66 °C for 12 min, and finally cooled back to room temperature. The measured changes in normalized conductivity and relative permittivity as a function of heating and cooling time are shown in figure 9. For comparison, equations (9) and (10) were used to calculate the expected  $\sigma(t)$  and  $\varepsilon'(t)$  based on the experimentally measured thermal history and the resulting theoretical curves were plotted in figure 9. A reasonable agreement (within approximately 10%) was observed between the experimental and theoretical curves describing the changes in dielectric properties of kidney during the thermal treatment.

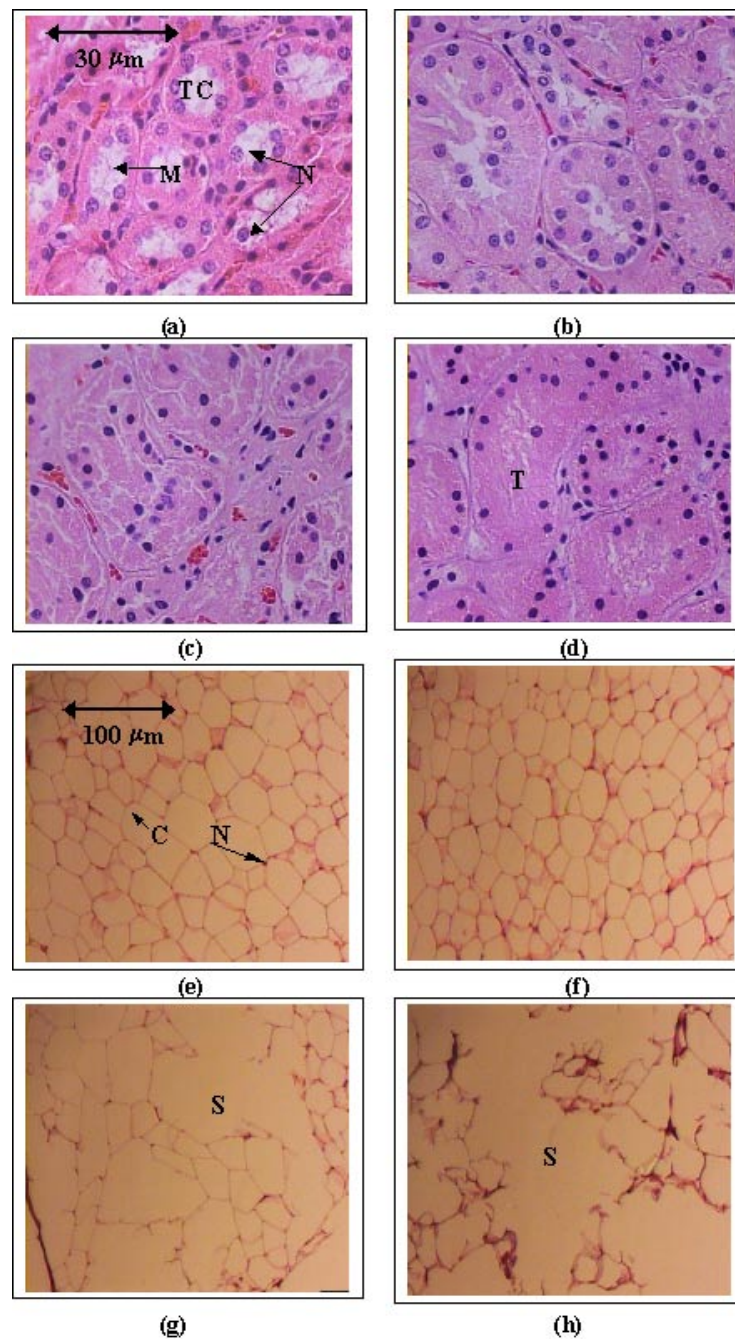


**Figure 10.** Representative light microscopy images (magnification:  $\times 500$  for kidney and  $\times 100$  for fat) of histological samples (H&E staining), illustrating (a) native, freshly excised porcine kidney (cortex); and the cortex structure after exposure at (b) 48.4 °C, (c) 55.1 °C, (d) 71.2 °C, and (e) native, freshly excised porcine fat (from peritoneal cavity); and the fat structure after exposure at (f) 60.3 °C, (g) 68.1 °C and (h) 78.4 °C.

(This figure is in colour only in the electronic version)

### 3.3. Histological and tissue gross appearance

Freshly excised porcine kidney cortex was red-pink in colour, moist and soft. After exposure to temperatures in the range 48–60 °C the tissue (after cooling) remained pink in colour and still moist. Inspection of the kidney samples treated at 64–71 °C revealed a whitening of the tissue and a slightly harder texture, whereas the samples treated at 78 °C were yellowish brown, shrunken and of a very hard texture.

Representative light microscopy images of the H&E stained samples illustrate the gradual irreversible thermal damage produced during exposure of renal tissue to high temperatures (figures 10(a)–(d)). For comparison, figure 10(a) displays a freshly excised cortex where tubular cells (TC) have a well-defined membrane (M) and healthy hypochromatic nuclei (N), and the apical membrane clearly defines the lumen. In samples exposed at 48 °C, a severe swelling of the cells is observed (figure 10(b)), forcing them to bulge into the lumen. Treatment at 55 °C (figure 10(c)) produces deformation of tubular cells accompanied by their detachment from the basement membrane. Here, the nuclei became slightly hyperchromatic (dark) and pyknotic (small). At 60 °C (not shown), most of the cells have an indistinct membrane, and the nuclei have moved towards the tubular membrane. Samples heated between 64 and 71 °C have the same histo-morphologic features (figure 10(d)): the tubules (T) are filled with an amorphous material, most likely resulting from cellular disintegration, with hyperchromatic and pyknotic nuclei containing condensed chromatin. Tubulorrexis (loss of tubular outline definition) was observed in samples heated at 78 °C (not shown), as they started to collapse and to fill the interstitium with products from dissolution of cellular organelles.

Freshly excised peritoneal fat tissue is white in colour and with a multi-layer packing structure that can be observed with the naked eye. After exposure to 48 °C or 60 °C, the fat appeared more compact and its colour turned to yellowish white. Some oily ‘tears’ were noticed at the surface. Fat tissue heated to 68 °C and 71 °C was yellowish, opaque and shiny, with a rubber-like texture. Samples exposed at 78 °C were hard, shrunken, slightly translucent and yellow in colour. A common characteristic of all samples heated between 68 °C and 78 °C was their ‘wet’ appearance due to the abundance of large oily droplets.

Histology of the native fat tissue revealed a meshwork of well-packed large adipocytes each characterized by a single large lipid inclusion (drop) surrounded by a thin rim of cytoplasm (C), with nuclei (N) compressed by the lipid mass to an eccentric position (figure 10(e)). Each space (S) represents the site of a single drop of lipid before its dissolution from the cell during H&E preparation. There were no significant histo-morphological differences between the samples heated at 48 °C (figure 10(f)) or 60 °C (not shown) and the unheated control sample. Samples treated at 68 °C (figure 10(g)), 71 °C (not shown) and 78 °C (figure 10(h)), contain evidence of thermal damage: abundant large spaces (S) resulting from dissolution of large areas of lipid droplets and areas with disorganized and deformed adipocytes.

## 4. Discussion

The frequency 460 kHz belongs to the so-called beta dispersion relaxation (between 1 kHz and few MHz) caused by the cellular structure of tissues, with poorly conducting membranes separating cytoplasm and extracellular fluid. The conductance  $G$  of bulk tissue is related to the ionic content and ionic mobility, the first dependent on tissue physiological state and the latter dependent on viscosity, water content and temperature (Pething and Kell 1987). Tissue electrical conductivity  $\sigma$  (calculated using equation (2)) is therefore assumed to be influenced by the same factors. The relative permittivity  $\epsilon'$  (calculated using equation (3)) describes the ability of tissue to store energy in response to an external field. This process is associated

with the polarization that arises from the charging of the cellular membranes and cellular organelles, through electrolytes (i.e. ions). The measured capacitance  $C$  reflects the ability of cellular membranes to limit the motion of bound charges. It was shown by Schwan and Foster (1980) that near the central frequency of the  $\beta$  dispersion range, tissues are expected to have positive temperature coefficients for both dielectric properties like those of electrolytes (i.e.  $+2\% \text{ }^\circ\text{C}^{-1}$ ). Our results regarding the temperature coefficients of dielectric properties showed a linear increase at increasing temperatures consistent with this theory. The only available values for comparison are those compiled by Duck 1990 up to  $40 \text{ }^\circ\text{C}$  which for kidney at  $0.1 \text{ MHz}$  were  $+0.9\% \text{ }^\circ\text{C}^{-1}$  for  $\sigma$ , and  $+0.8\% \text{ }^\circ\text{C}^{-1}$  for  $\epsilon'$ . For fat, data available at  $50 \text{ MHz}$  are  $1.7\% \text{ }^\circ\text{C}^{-1}$  for  $\sigma$  and at  $200 \text{ MHz}$  are  $+1.3\% \text{ }^\circ\text{C}^{-1}$  for  $\epsilon'$ . These values are in reasonable agreement with the values derived here (table 1). However, although we fitted a constant temperature coefficient we noted that our data (figure 7) showed a slight breakpoint at  $72 \text{ }^\circ\text{C}$  such that  $\epsilon'(30)/\epsilon'(45)$  and  $\sigma(30)/\sigma(45)$  are shifted slightly higher above this temperature. This may be explained if the temperature coefficient for completely denaturated (coagulated or melted) tissue is different from that for unheated tissue.

In this work, we separated reversible (temperature dependent) effects from irreversible effects due to structural events. For kidney permittivity these two effects competed, the latter effect being dominant and leading to a gradual decrease in permittivity. An increase in the conductivity of kidney and the conductivity and permittivity of fat after  $t_{\text{structural}}$  was observed. Both dielectric properties of renal tissue and fat reached a plateau as the thermal denaturation (coagulation or melting) of tissue was complete. However, differences in the time–temperature dependence for different types of tissue might be expected. For example, Ryan *et al* (1997) showed no further changes in the electrical conductivity of muscle at  $500 \text{ kHz}$  after thermal equilibrium had been reached for temperatures between  $30 \text{ }^\circ\text{C}$  and  $60 \text{ }^\circ\text{C}$  suggesting that the dielectric properties of muscle tissue have dependence on temperature but no changes due to coagulation. Chin and Sherar (2003) have observed a similar lack of structural effect in the dielectric properties of rat prostate at  $915 \text{ MHz}$ , although they did observe permanent changes in dielectric properties of bovine liver at the same frequency (Chin and Sherar 2001).

Our analysis demonstrated that permanent changes in dielectric properties of kidney and fat can be modelled by a single first-order Arrhenius process. The activation energies derived in our study (table 2) are in a similar range to those reported by McRae and Esrick (1993) for the changes in electrical resistivity of *ex vivo* skeletal muscle (below  $40 \text{ MHz}$ ) during hyperthermia ( $36.1$  and  $58.3 \text{ kcal mol}^{-1}$  above and below  $43 \text{ }^\circ\text{C}$ , respectively). They are also in the same range as the values of  $70.7 \text{ kcal mol}^{-1}$  for permittivity and  $60.1 \text{ kcal mol}^{-1}$  for conductivity of *ex vivo* bovine liver at  $915 \text{ MHz}$  during exposure at high temperatures (Chin and Sherar 2001).

In this work, the correlation between dielectric measurements and histological findings suggests that the permanent changes in  $\epsilon'$  and  $\sigma$  of renal tissue, at temperatures below  $55 \text{ }^\circ\text{C}$ , may be due to small membrane breaks and swelling. Cellular swelling, progressive membrane breakage and histolysis found at the end of a hyperthermic treatment (up to  $46 \text{ }^\circ\text{C}$ ) were similarly considered as the possible cause of the permanent increase in conductivity and decrease in permittivity of EMT6 tumours (McRae and Esrick 1992). At temperatures above  $55 \text{ }^\circ\text{C}$ , renal tubular cells shrunk and their membranes collapsed. The tubules appeared filled with an amorphous material probably resulting from the dissolution of the membranes and organelles. These events led to a further increase in conductivity as more ionic pathways became available, and to a decrease in permittivity perhaps as the bounded charges became unbounded. After exposure to temperatures between  $64 \text{ }^\circ\text{C}$  and  $71 \text{ }^\circ\text{C}$  the conductivity values of kidney after cooling were all similar, in agreement with histological analysis where identical thermally induced changes in these samples were observed. Similar histological results of the

thermal damage in porcine kidney were demonstrated by Watkin *et al* (1997) and Elbadawi *et al* (1976).

The thermal injury induced in fat at high temperatures is likely due to a process of *melting* of its fatty acid components. As the target temperature was increased, more *islands* of lipid material (with larger areas suggesting membranes' breakdown and dissolution) were observed indicating that a melting process had occurred. The observed increase in both dielectric properties of fat was unexpected from energy consideration. The sum of real part  $\epsilon'$  (reflecting the energy stored in tissue) and imaginary part  $\epsilon'' = \sigma/2\pi\nu\epsilon_0$  part (reflecting the energy loss in tissue) of the complex dielectric permittivity ( $\epsilon^* = \epsilon' - j\epsilon''$ ) is constant. Therefore, if one component increases the other component is expected to decrease. Interestingly, Kyber *et al* (1992) observed similar behaviour in the dielectric properties of porcine fat at cryogenic temperatures (140 K) where, both real ( $\epsilon'$ ) and imaginary ( $\epsilon''$ ) parts were found to decrease with decreasing temperature.

The values derived for critical temperatures (table 2) suggest that the fat tissue is more thermally resistant than kidney tissue (i.e. after a 10 min exposure at approximately 63 °C, the kidney tissue is coagulated whereas the changes in fat tissue are still negligible).

These results should be useful for the treatment planning of the radio-frequency thermal therapy because changes in dielectric properties affect the energy absorbed by the tissue from the RF source. Incorporation of the dielectric changes, described by equations (9)–(12), into a nonlinear mathematical model of the RF thermal therapy should result in more accurate predictions of temperature rise expected in the tissue and the subsequent thermal damage. Further work is necessary in order to measure the dielectric properties of kidney *tumours* at 460 kHz during heating.

## 5. Conclusion

We demonstrated a time–temperature dependence of the dielectric properties of *ex vivo* porcine kidney and fat at 460 kHz during heating at high temperatures. Results revealed two major contributions: a reversible, temperature-dependent effect and a permanent effect due to structural changes (e.g. protein coagulation, fatty acid melting) in tissues during heating. Our study demonstrated that the Arrhenius formalism can be used to model the structural changes in dielectric properties of kidney and fat, and that mathematical equations can be used to describe the change in dielectric properties as a result of any thermal history. These mathematically described changes in dielectric properties could be incorporated into theoretical calculations to predict tissue temperature during RF heating in kidney and surrounding fat.

## Acknowledgments

The authors are grateful to Ms Diana Birlle (MD Pathologist) and to Mrs Anoja Giles for their assistance with the histology analysis and to Mr Arthur Worthington for helping to build the experimental apparatus. This work was supported in part by the Kidney Foundation of Canada.

## References

- Chin L and Sherar M D 2001 Changes in dielectric properties of *ex vivo* bovine liver at 915 MHz during heating *Phys. Med. Biol.* **46** 197–211
- Chin L and Sherar M D 2003 Changes in the dielectric properties of rat prostate *ex vivo* at 915 MHz during heating *Int. J. Hyperth.* submitted
- Duck F A 1990 *Physical Properties of Tissue, A Comprehensive Reference Book* (London: Harcourt Brace)

- Elbadawi A, Linke C A, Carstensen E L and Fridd C W 1976 Histomorphologic features of ultrasonic renal injury *Arch. Pathol. Lab. Med.* **100** 199–205
- Gabriel S, Lau R W and Gabriel C 1996 The dielectric properties of biological tissues: II. Measurements in the frequency range 10 Hz to 20 GHz *Phys. Med. Biol.* **41** 2251–69
- Gervais D A, McGovern F J, Wood B J, Goldberg N S, McDougal S W and Mueller P R 2000 Radio-frequency ablation of renal cell carcinoma: early clinical experience *Radiology* **217** 665–72
- Haemmerich D, Staelin T S, Tungjitkusolmun S, Lee F T, Mahvi D M and Webster J G 2001 Hepatic bipolar radio-frequency ablation between separated multiprong electrodes *IEEE Trans. Biomed. Eng.* **48** 1145–52
- Hart F X and Dunfee W R 1993 *In vivo* measurement of the low-frequency dielectric spectra of frog skeletal muscle *Phys. Med. Biol.* **38** 1099–112
- Hart F X, Schmidt V, Ray L and Shrum E 1998 Measurement of the activation enthalpies of ionic conduction in apples *J. Mater. Sci.* **33** 3919–25
- Henriques F C 1947 Studies of thermal injury: V. The predictability and the significance of the thermally induced rate processes leading to irreversible epidermal injury *Arch. Pathol.* **5** 459–502
- Kato H and Ishida T 1987 Development of an agar phantom adaptable for simulation of various tissues in the range 5–40 MHz *Phys. Med. Biol.* **32** 221–6
- Kyber J, Hansgen H and Pliquet F 1992 Dielectric properties of biological tissue at low temperatures demonstrated on fatty tissue *Phys. Med. Biol.* **37** 1675–88
- Labonté S 1994 A computer simulation of radio-frequency ablation of the endocardium *IEEE Trans. Biomed. Eng.* **41** 883–90
- Martinsen O G, Grimnes S and Schwan H P 2002 Interface phenomena and dielectric properties of biological tissue *Encyclopedia of Surface and Colloid Science* ed A Hubbard (New York: Marcel Dekker) pp 2643–52
- McRae D A and Esrick M A 1992 The dielectric parameters of excised EMT-6 tumours and their change during hyperthermia *Phys. Med. Biol.* **37** 2045–58
- McRae D A and Esrick M A 1993 Changes in electrical impedance of skeletal muscle measured during hyperthermia *J. Int. Hyperth.* **9** 247–61
- Meijerink R, Essenpreis M, Pickering J W, Massen C H, Mills T N and van Gemert M J C 1995 Rate process parameters of egg white measured by light scattering *Laser Induced Interstitial Thermoablation* ed G Muller and A Rogan (Bellingham, WA: SPIE Optical Engineering Press) pp 66–80
- Michaels M J, Rhee H K, Mourtzinou A P, Summerhayes I C, Silverman M L and Libertino J A 2002 Incomplete renal tumor destruction using radio frequency interstitial ablation *J. Urol.* **168** 2406–10
- Molckovsky A and Wilson B C 2001 Monitoring of cell and tissue responses to photodynamic therapy by electrical impedance spectroscopy *Phys. Med. Biol.* **46** 983–1002
- Pearce J and Thomsen S 1995 Rate process analysis of thermal damage *Optical-Thermal Response of Laser-Irradiated Tissue* (New York: Plenum) pp 561–605
- Pethig R and Kell D B 1987 The passive electrical properties of biological systems: their significance in physiology, biophysics and biotechnology *Phys. Med. Biol.* **32** 933–70
- Rendon R A, Gertner M R, Sherar M D, Asch M R, Kachura J R, Sweet J and Jewett M A S 2001 Development of a radiofrequency based thermal therapy technique in an *in vivo* porcine model for the treatment of small renal masses *J. Urol.* **166** 292–8
- Rendon R A, Kachura J R, Sweet J, Gertner M R, Sherar M D, Robinette M, Tsihlias J, Trachtenberg J, Sampson H and Jewett M A S 2002 The uncertainty of radiofrequency (RF) treatment of renal cell carcinoma (RCC): findings at immediate and delayed nephrectomy *J. Urol.* **167** 1587–92
- Ryan T P, Platt R C, Dadd J S and Humphries S 1997 Tissue electrical properties as a function of thermal dose for use in a finite element model *Adv. Heat Transfer Biotechnol.* **37** 167–71
- Schwan H P 1963 Determination of biological impedances *Phys. Tech. Biol. Res.* **6** 323–407
- Schwan H P and Foster K R 1980 RF-field interactions with biological systems: electrical properties and biophysical mechanisms *Proc. IEEE* **68** 104–13
- Skinner M G, Everts S, Reid A D, Vitkin I A, Lilge L and Sherar M D 2000 Changes in optical properties of *ex vivo* rat prostate due to heating *Phys. Med. Biol.* **45** 1375–86
- Strohbehn J 1983 Temperature distributions from interstitial RF electrode hyperthermia systems: theoretical prediction *Int. J. Radiat. Oncol.* **9** 1655–67
- Thomsen S 2000 Qualitative and quantitative pathology of clinically relevant thermal lesions *Crit. Rev. Opt. Sci. Technol.* **75** 425–58
- Van de Kamer J B, Van Wieringen N, De Leeuw A A C and Lagendijk J J W 2001 The significance of accurate dielectric tissue data for hyperthermia treatment planning *J. Int. Hyperth.* **17** 123–42
- Watkin N A, Morris S B, Rivens I H and Ter Haar G R 1997 High-intensity focused ultrasound ablation of the kidney in a large animal model *J. Endourol.* **11** 191–6